

Methodology: Permian Methane Analysis Project (PermianMAP)

Data Collection and Analysis

Last Update: Aug. 5, 2020

Aerial Surveys: Scientific Aviation

Scientific Aviation quantifies methane emissions at various spatial scales from a cluster of a few well pads to the entire study area using the aerial mass balance approach. In summary, a Mooney aircraft equipped with a Picarro CRDS methane analyzer is flown around the target area to measure upwind and downwind methane concentration. The traditional mass balance approach or Gauss's law variation is used to estimate methane emissions based on wind speed and direction and the difference in upwind and downwind integrated methane concentration. These emission estimates represent snapshots of total emissions from the areas circumscribed by the plane. Based on earlier controlled release experiments, the detection limit of the mass balance approach can be as low as 5–10 kg CH₄/hr, but the exact detection limit is highly dependent on dynamic parameters such as upwind methane concentration. Additional details and references about Scientific Aviation's approach can be found at: <http://www.scientificaviation.com/methods/>.

For PermianMAP, Scientific Aviation is being deployed for four types of measurements: regional mass balances, box mass balances, site cluster mass balances, and flare combustion efficiency. Regional mass balance flights occur opportunistically during optimal wind conditions, such as consistent wind direction; these long flights measure methane emissions around the entire study area or other large regions to estimate total methane emissions. Box mass balances occur systematically around 25 pre-defined 20x20 km boxes within our 100x100 km study area; these measurements will be repeated in each study area to determine how the coarse spatial distribution of emissions changes over time. Most aerial measurements are site cluster measurements that the aircraft measures with 1–2 km radius spiral flights to measure the plume from near ground level to its vertical extent. These areas are selected using two strategies based on the 20x20 km boxes: randomly selected locations and randomly selected single-operator clusters. For each 20x20 km box, five to ten 2x2 km sub-grids are randomly selected for 1 – 2 km circular mass balances centered on the sub-grids; these areas often contain wells from multiple operators. For the second approach, we pre-defined irregular shapes in each 20x20 km based on a geospatial analysis that clustered wells into single operator groups. For each 20x20 box, several of these single operator areas are randomly selected for mass balance measurements. The final approach is quantifying flare combustion efficiency. For flare measurements, the aircraft flies through flare plumes to measure concentrations of methane and carbon dioxide; the ratio of these species will be used to estimate the percentage of methane combusted by the flare.

PermianMAP publishes by Scientific Aviation data for any measurements that have passed quality assurance. New data will be added from both additional flights and quality assurance of existing data. While a best effort has been made to provide accurate emission estimates, all data should be considered preliminary and subject to change.

Attributing Wells to Emission Events

We determine which wells are associated with a given emission event using several well characteristics. The well must have been actively in operation or actively producing during our study period (October 2019 – present) and must have a first production date prior to the given emission event. This allows us to maintain up-to-date well data while avoiding associating new wells with older emission events.

Ground Surveys: University of Wyoming

The University of Wyoming (UW) team quantifies site-level methane and VOC emissions using two vehicle-based approaches: Other Test Method 33A (OTM) and the transect method. OTM is an inverse Gaussian dispersion method developed by the US EPA. In summary, a vehicle equipped with a pollutant sensor and 3D sonic anemometer is deployed 40–200 meters downwind of an emission source for approximately 20 minutes at a stationary location near the plume centerline. Site-level emission rates are estimated by fitting concentration and wind data to a Gaussian curve; more methodological details on OTM 33A can be found in footnotes 1 to 3^{1,2,3}. The transect method uses the same vehicle-based measurement platform, but samples the plume as the vehicle drives back and forth on a downwind road in a direction transverse to wind⁴. The precision of OTM and the transect method (for 10+ passes) have been estimated to be +233%/-41% and +170%/-50%, respectively^{4,5}.

In January 2020, UW deployed their mobile air quality laboratory to the study area to perform OTM and transect measurements at randomly selected well pads and tank batteries. Methane and speciated VOCs were measured continuously with a Picarro CRDS and PTR-TOF-MS; additional details on laboratory instrumentation can be found in Robertson et al 2017 and Edie et al 2020^{4,6}. Site selection followed a pseudo-random process that accounted for the methodological constraint of downwind public road access. We randomly selected several 20x20 km areas within our gridded 100x100 km access, excluding any area with limited public roads. The UW team randomly selected sites within each 20x20 km area for OTM and/or transect measurements that were downwind of the current wind direction. In addition to quantifying emissions, the UW team used a FLIR camera to inspect the site for emissions from the fence line. At some sites, a canister air sample was collected for VOC analysis to supplement PTR-TOF-MS data. For sites where it was confirmed that the mobile laboratory was downwind of the site, but no enhanced methane was detected for at least 10 minutes, emissions were reported as below detection limit, which has been estimated as 0.036 kg CH₄/hr for the OTM method².

Flaring Survey

EDF compiled a list of potential locations of recently active flares in the Permian region (Delaware and Midland Basins) based on a geospatial analysis of the [SkyTruth Global Flaring Dataset](#). The SkyTruth data includes probable locations of oil and gas flares detected as heat sources by the Visible Infrared Imaging Radiometer Suite (VIIRS) instrument on the NOAA Suomi NPP satellite. To account for spatial uncertainty of SkyTruth flare locations, we spatially joined their individual flare detections from 10/1/2019 to 1/31/2020 using a 100-meter buffer distance; the centroid latitude/longitude of the 1,014 joined detections were defined as likely locations of recently active O&G flares.

[Leak Surveys Incorporated](#) (LSI), a leak detection company specializing in aerial optical gas imaging, was provided a list of 573 potential active flare locations from the original set of 1,014. Site selection balanced representativeness and efficiency by defining one contiguous, high flare density area in each basin that could be surveyed in a total of approximately five days. For the Delaware, we selected 323 locations corresponding to part of the main PermianMAP study area defined by the NW and SE corners 32.325° N, 103.822° W and 31.417° N, 103.202° W, plus three additional flares on University Lands located within 6 km of the study area. For the Midland, we selected 250 locations from the two counties with the highest flare counts: Midland and Martin.

LSI surveyed these locations with a custom infrared camera (IR) deployed in a R44 helicopter. Flare locations were identified with a latitude/longitude and unique flare ID. During the week of February 17, 2020 (Survey 1), LSI surveyed the selected 573 potential flare locations to determine the presence of a flare; if a flare was identified near the spatial coordinates, LSI recorded 15 – 30 seconds of both visual spectrum and IR video of the flare and nearby equipment. For flares with apparent combustion issues, LSI recorded an additional 30 – 60 seconds of footage of the flare plume from multiple angles to provide visual evidence of flare status. For each flare, LSI assigned a qualitative assessment of the apparent flare status at the time of survey from four categories: inactive and unlit with no emissions (inactive); active, lit, and operating properly (operational); active and lit but with operational issues such as incomplete combustion or excessive smoke (malfunction); or active, unlit, and venting methane (unlit and venting). If multiple flares were present at approximately the same distance from the reported coordinates, then the LSI randomly select a flare to assign to the Flare ID. If no active or inactive flares are visible from the reported coordinates, then the team reported no flare was present at the location.

During the week of March 23, 2020 (Survey 2), LSI was deployed for a follow-up survey at 337 flare locations: all of the malfunctioning or unlit flares from Survey 1 plus a random selection of half the operational or inactive flares from the first survey. LSI used a similar protocol as the first survey, but only recorded video for flares with a malfunctioning or unlit status. Additionally, LSI was deployed to systematically survey all O&G flares in a 20 x 20 km box defined by the NW and SE corners 31.780° N, 103.406° W and 31.596° N, 103.199° W. The systematic survey results, which are not included in the current analysis, will be used in later analyses to assess if the flares based on the VIIRS dataset are representative of the full population; it is likely the satellite-detected flares are larger on average and therefore may have different performance than smaller flares.

A third flaring survey occurred from Jun 22 – July 1, 2020 with a similar methodology to the second survey for repeated observations of problematic flares and random sampling of the identified flares. The systematic survey was also repeated during Survey 3.

For Survey 1, LSI found 337 flares at the provided locations, 312 of which were active during the survey. About 11% of flares had issues that could cause abnormally high methane emissions: 7% were lit but with combustion issues, while 4% were unlit and venting. For Survey 2, the analysis accounts for the sampling strategy bias towards malfunctioning/unlit flares by adding predicted results from the 50% of operational/inactive flares that were not re-surveyed. After this adjustment, the second survey results are similar to the first survey: about 12% of flares had issues (7% combustion issues, 5% unlit). Twenty-five percent (9/36) of flares were observed to have issues during both surveys. Including approaches for estimating the performance of unsampled flares, the third survey found similar results with 11% of flares malfunctioning and 4.5% to be unlit and venting – including two flares which were found to be malfunctioning during the course of all three surveys (Flare ID 448 and 630).

To estimate methane emissions from flaring, we used our qualitative flare performance data and reasonable assumptions about the combustion efficiency of operational, malfunctioning, and unlit flares to estimate overall combustion efficiency; and then applied that data to estimated flared volumes in 2019 based on an analysis of VIIRS data. Gas flared volumes were estimated using nighttime fire and flare data observed by VIIRS instrument on board the Suomi National Polar-Orbiting satellite. Daily VIIRS data for January to December 2019 were downloaded from https://eogdata.mines.edu/download_viirs_fire.html. We filtered the VIIRS data for observations with flare source temperatures in the range of 1400 to 2500 K, which are representative of gas flares. The gas flaring volumes were estimated using the empirical relationship derived by the Elvidge et al. 2015⁷ equation $V_{\text{annual}} = 0.0274RH^{\wedge}$ where V_{annual} is the gas flared volume in bcm and RH^{\wedge} is the average adjusted radiant heat of the observed flares, adjusted to account for the observed non-linearity in the relationship between flared gas volumes and radiant heat parameters. Using this approach, mean flaring volumes in the Permian Basin are estimated at 7.9 bcm (or 280 bcf) in 2019, with 6.5 bcm (230 bcf) in the Texas portion of the Permian and the remainder (1.4 bcm or 49 bcf) in the New Mexico Permian Basin.

We assume that operational flares perform at the EPA default combustion efficiency of 98%, which means 2%

of the methane sent to the flare is emitted rather than being combusted to carbon dioxide. Unlit flares have a combustion efficiency of 0% since all the methane is emitted unburnt. For the flares that were lit, but with apparent combustion issues, we assumed 90% combustion efficiency. These assumptions lead to an overall combustion efficiency of 93%, which means 7% of flared methane is emitted (Table 1). Applying 93% combustion efficiency to the 280 bcf of gas flared in the Permian in 2019 (assuming 80% CH₄ content) results in annual methane emissions of approximately 300,000 metric tons from flaring in the Permian; unlit flares account for about 65% of these emissions, while operational and poorly combusting flares account for about 15 and 10%, respectively. Based on the state-specific flared gas volumes, Texas and New Mexico are responsible for about 250,000 and 50,000 MT CH₄, respectively. In comparison, applying the EPA default assumption combustion efficiency of 98% results in about 80,000 – 90,000 metric tons CH₄ emissions. Our emissions estimate is about 3.5 times higher than alternative estimates based on EPA assumptions of combustion efficiency. EPA publishes two separate estimates of Permian flaring methane emissions, which incorporates the 98% combustion efficiency but different gas flared data. The [2020 Greenhouse Gas Inventory](#) reports 2018 Permian Basin methane emissions of 12,100 metric tons CH₄ from associated gas flaring, plus 8,500 MT and 4,600 MT from associated gas venting and miscellaneous production flaring, respectively. The [Greenhouse Gas Reporting Program](#) reports 18,800 MT CH₄ from Permian Basin onshore production facilities.

Total	Survey 1	Survey 2	Survey 3	Average
Operational	276	147	237	
Inactive	25	0	62	
Combustion Issue	23	9	18	
Unlit and Venting	13	10	12	
Not surveyed	94	265	102	
Active Flares	312	166	267	
Malfunctioning (CI + U&V)	36	19	30	
% Malfunctioning	11.5%	11.4%	11.2%	11.4%
% Unlit and Venting	4.2%	6.0%	4.5%	4.9%

Data Availability

All data collected through the surveys, including estimated emission rates and associated uncertainty, are available. The project website will be updated soon to include a data download feature. For immediate assistance, please contact permianmap@edf.org.

Additional Data Sources

The project's analyses and data presentation (on PermianMAP.org) includes additional data on wells and midstream facilities from the following sources:

Texas Railroad Commission:

https://www.rrc.state.tx.us/about-us/resource-center/research/data-sets-available-for-download/#digital_map

New Mexico Oil Conservation Division*:

<http://www.emnrd.state.nm.us/OCD/ocdgis.html>

For operator name, well type, production status, and average daily production, the project used proprietary data provided by Enverus:

<https://www.enverus.com>

Tank battery locations are based on satellite imagery analysis by Descartes Labs.

<https://www.descarteslabs.com/>

The processing plants locations are from the EPA GHG Reporting Program:

<https://ghgdata.epa.gov/ghgp/main.do>

* Note that New Mexico and Texas well data is updated on a monthly basis.

Regional Emissions Estimate: Study Area Loss Rate

On March 9, Scientific Aviation flew two transects around the full 10,000 km² study area during meteorological conditions of consistent, westerly winds. Measured methane enhancement (concentration in parts per billion over background) along the flight paths are shown in Figure 1 below. Methane concentrations are substantially higher in the eastern transect, which is due to methane emissions from within the study area dispersing downwind. Researchers at The Pennsylvania State University used two different approaches to estimate total methane emissions: the mass balance method and atmospheric transport modeling. The traditional mass balance method, described in Scientific Aviation's methods, uses the wind speed and direction and the difference in integrated methane concentration between upwind and downwind transects to estimate emissions. Based on the traditional mass balance approach, study area emissions were ~160,000 kg CH₄/hr. Atmospheric transport modeling optimizes the fit of measured and modeled methane concentrations based on a current best estimate, spatially resolved emission inventory (prior) and meteorological data. The Weather Research and Forecasting – Chemistry model (WRF-CHEM) was used to compute the dispersion of methane based on March 9 meteorological conditions. The prior inventory, which we developed from EPA data and known O&G infrastructure, estimates study area emissions are 54,000 kg/hr, but there is a poor fit between the simulated and observed methane concentrations (Figure 1, bottom left panel).

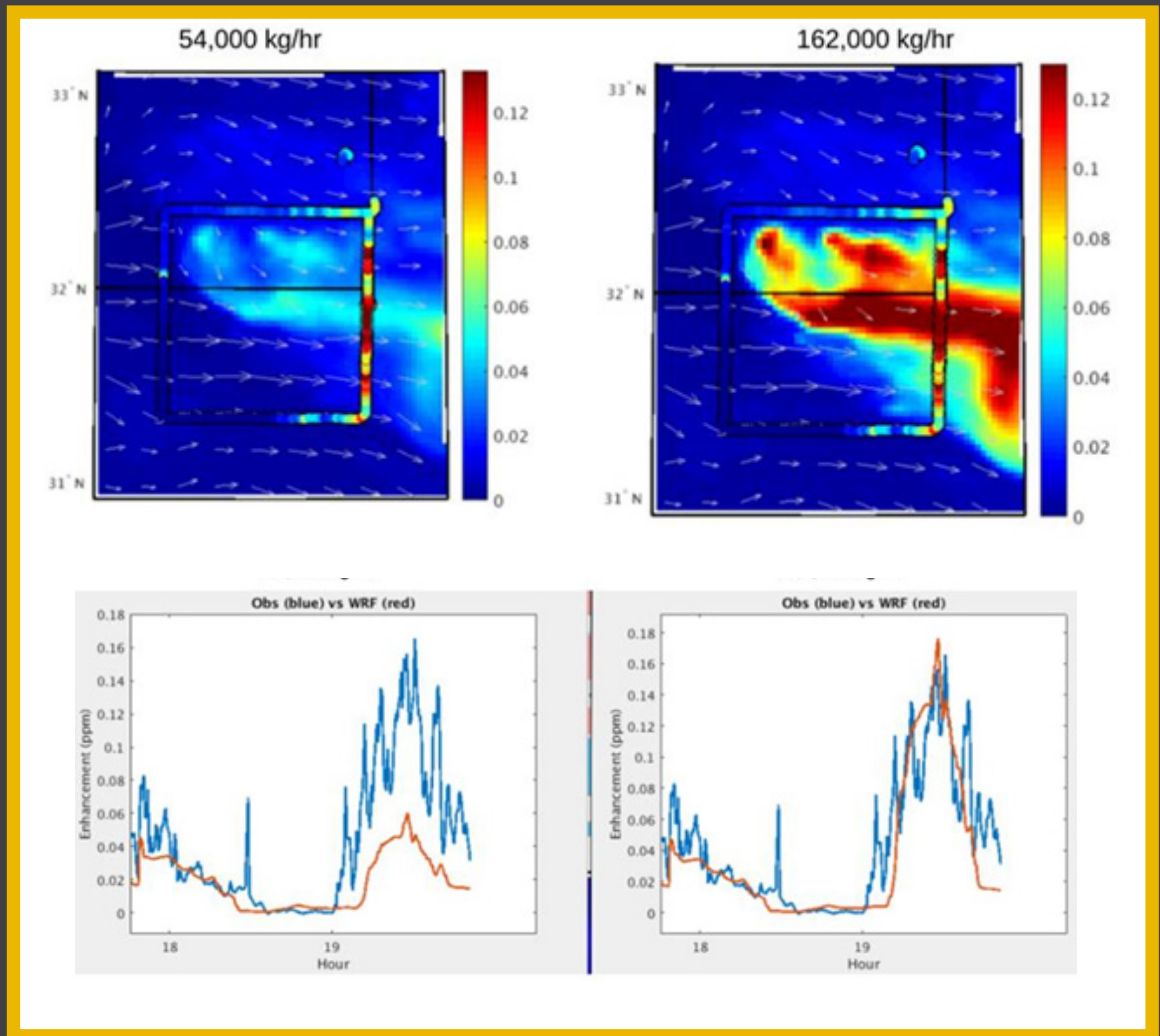
If the prior inventory is tripled to 162,000 kg/hr, then there is close fit between measured and modeled concentrations (bottom right panel). This optimized inventory (prior) is the best estimate of emissions based on atmospheric transport modeling. The close agreement between these two approaches supports that methane emissions on March 9 were approximately 160,000 kg/hr. Scientific Aviation also has completed two other mass balance flights of the study region, which had higher uncertainty due to meteorological conditions, but preliminary data indicate are of similar magnitude to the March 9 flight.

To calculate a loss rate (methane emissions normalized to methane production) in our study area, we use Enverus data to determine all wells in the study area with production during October 2019 – February 2020. As of April 1, 2020, January 2020 was the most recent month with nearly complete production data. Therefore, we selected January 2020 production as most representative of the March 9 flight. We used ArcGIS to select and aggregate January daily average gas production within the flight path. We converted this gas production value of ~7,300,000 Mcf/day into a methane production value of 4,672,000 kg CH₄/hr based on assumptions of 80% methane content and 19.2 kg CH₄/Mcf. **Therefore, 162,000 kg CH₄/hr is equivalent to about 3.5% of methane production.**

Our loss rate estimate for the Permian Basin is substantially higher than the national average. The EPA Draft 2020 Greenhouse Gas Inventory (GHGI) estimates national O&G supply chain methane emissions are 7.1 Tg, equivalent to approximately a 1.3% loss rate. Our study area contains limited transmission and local distribution, so it is more appropriate to compare to only the production, gathering, and processing segments — which is ~1.1% in draft 2020 GHGI. **Consequently, our measurement-based estimate is about 3 times higher than the EPA inventory.** In comparison, Alvarez et al 2018 used site- and basin-level data to estimate national average oil and gas supply chain methane emissions are 13 Tg, or a 2.3% loss rate; for production, gathering, and processing, the loss rate is ~2.0%. Accordingly, the Permian loss rate is about 75% higher than this current best estimate of national emissions.

Figure 1.

Prior (left) and posterior (right) modeled and measured methane enhancement (concentration in parts per million over background) for the March 9 flight. The colors in the square perimeter represent measured methane enhancement from Scientific Aviation's flight around the study area. The bottom figures show that the prior inventory of 54,000 kg/hr does not match observed enhancement, but tripling the prior emissions 162,000 kg/hr causes the modeled and observed concentration to match.



Uncertainty, Detection Limits, and Scale

As with any emission estimate technique, the approaches used by Scientific Aviation and University of Wyoming have both uncertainty and minimum detection limits. Uncertainty refers to the accuracy (how close to the actual value) and precision (consistency) of measurements. The minimum detection limit (MDL) is the smallest emission rate that an approach can quantify with enough precision to determine if it is statistically significant from zero. The uncertainty and MDL of the mass balance, OTM 33a, and transect approach have been tested with two basic techniques: 1) controlled release tests, and 2) uncertainty propagation. Single blind controlled releases can be used to empirically test the accuracy, precision, and probability of detection at different emission rates and conditions. Uncertainty propagation uses statistical techniques to estimate total uncertainty of an estimate from the uncertainty of input parameters such as wind speed. Based on controlled releases, Scientific Aviation's mass balance approach for small areas can detect emissions as small as 5–10 kg CH₄/hr with 10% uncertainty during optimal conditions. However, based on uncertainty propagation, the Permian project measurements have a median uncertainty closer to ±60% with few measurements less than 40 kg/hr being statistically significant from zero. This higher uncertainty and detection limit are likely due to the high density of methane sources, which increases the variability of upwind methane concentrations. OTM 33A can detect much smaller emissions down to 0.036 kg CH₄/hr with +233%/-41% uncertainty. Although the OTM 33A has relatively poor precision, controlled tests have shown it has little bias, which means it can be used to accurately characterize a population with a large enough sample size.

On the PermianMAP website (permianmap.org), we present measured areas using a colored scale with five bins based on absolute emission rates in kg CH₄/hr: 1) Red: >1000 kg/hr; 2) Orange: 100 – 1000 kg/hr; 3) Yellow: 2 – 200 kg/hr; 4) White: <2 kg/hr; and 5) Grey: Below Detection. For context, previous studies such as Omara et al 2018 and Alvarez et al 2018 estimate that the average U.S. well emits between 1 – 2 kg/hr. The grey bin of “below detection” indicates measurements that could not determine if there were emissions above zero. The detection limit varies greatly between the types of approaches. For Scientific Aviation measurements, preliminary data indicate the detection limit may be as high as 40 kg/hr in the complex Permian environment. In contrast, UW measurements have a detection limit near 0.036 kg/hr. Therefore, there is high confidence that UW below detection sites have low emissions, but it is possible that Scientific Aviation sites below detection could have relatively high emissions that were unable to be quantified due to issues such as interfering sources.

¹ United States Environmental Protection Agency. 2014. Draft Other Test Method 33: Geospatial Measurement of Air Pollution, Remote Emissions Quantification. <https://www3.epa.gov/ttnernc01/prelim/otm33.pdf>

² Brantley, H.L., Thoma, E.D., Squier, W.C., Guven, B.B. and Lyon, D., 2014. Assessment of methane emissions from oil and gas production pads using mobile measurements. *Environmental science & technology*, 48(24), pp.14508-14515. <https://pubs.acs.org/doi/abs/10.1021/es503070q>

³ Robertson, A.M., Edie, R., Snare, D., Soltis, J., Field, R.A., Burkhart, M.D., Bell, C.S., Zimmerle, D. and Murphy, S.M., 2017. Variation in methane emission rates from well pads in four oil and gas basins with contrasting production volumes and compositions. *Environmental science & technology*, 51(15), pp.8832-8840. <https://pubs.acs.org/doi/abs/10.1021/acs.est.7b00571>

⁴ Caulton, D.R., Li, Q., Bou-Zeid, E., Fitts, J.P., Golston, L.M., Pan, D., Lu, J., Lane, H.M., Buchholz, B., Guo, X. and McSpirtt, J., 2018. Quantifying uncertainties from mobile-laboratory-derived emissions of well pads using inverse Gaussian methods. *Atmospheric Chemistry and Physics*, 18(20), pp.15145-15168. <https://www.atmos-chem-phys.net/18/15145/2018/>

⁵ Edie, R., Robertson, A.M., Field, R.A., Soltis, J., Snare, D.A., Zimmerle, D., Bell, C.S., Vaughn, T.L. and Murphy, S.M., 2020. Constraining the Accuracy of Flux Estimates Using OTM 33A. *Atmospheric Measurement Techniques*, 13, pp.341-353. <https://www.atmos-meas-tech.net/13/341/2020/amt-13-341-2020.pdf>

⁶ Edie, R., Robertson, A.M., Soltis, J., Field, R.A., Snare, D., Burkhart, M.D., and Murphy, S.M., 2020. Off-Site Flux Estimates of Volatile Organic Compounds from Oil and Gas Production Facilities Using Fast-Response Instrumentation. *Environmental Science & Technology*, 54(3), pp. 1385 – 1394. <https://doi.org/10.1021/acs.est.9b05621>

⁷ Elvidge, C.D.; Zhizhin, M.; Baugh, K.; Hsu, F.-C.; Ghosh, T. Methods for Global Survey of Natural Gas Flaring from Visible Infrared Imaging Radiometer Suite Data. *Energies* 2016, 9, 14. <https://doi.org/10.3390/en9010014>